Use of dielectric functions in the theory of dispersion forces

Je-Luen Li,[1,2] Jaehun Chun,[3] Ned S. Wingreen,[2,4] Roberto Car,[1] Ilhan A. Aksay,[3] and Dudley A. Saville[3]
[1]*Department of Chemistry, Princeton University, Princeton, New Jersey 08544, USA*
[2]*NEC Laboratories America, Incorporated, 4 Independence Way, Princeton, New Jersey 08540, USA*
[3]*Department of Chemical Engineering, Princeton University, Princeton, New Jersey 08544, USA*
[4]*Department of Molecular Biology, Princeton University, Princeton, New Jersey 08544, USA*
(Received 23 August 2004; revised manuscript received 30 November 2004; published 21 June 2005)

The modern theory of dispersion forces uses macroscopic dielectric functions $\epsilon(\omega)$ as a central ingredient. We reexamined the formalism and found that at separation distance <2 nm the full dielectric function $\epsilon(\omega,\mathbf{k})$ is needed. The use of $\epsilon(\omega,\mathbf{k})$ results in as much as 30% reduction of the calculated Hamaker constants reported in the current literature. At larger distances, the theory reduces to the traditional method, which uses dielectric functions in the long-wavelength limit. We illustrate the formalism using the example of interaction between two graphite slabs. This example is of importance for intercalation and exfoliation of graphite and for the use of exfoliated graphite in composite materials. The formalism can also be extended to study anisotropic van der Waals interactions.

DOI: 10.1103/PhysRevB.71.235412 PACS number(s): 68.03.Cd

I. INTRODUCTION

The most common way to approximate van der Waals forces is by a pairwise summation over all involved particles.[1] This approach facilitates efficient computation but neglects many-body effects present in dense media, such as liquids or solids. A more satisfactory scheme was developed in the 1950s by Lifshitz[2] and Dzyaloshinski *et al.*[3] This "modern" theory can be cast in the form of sums over electromagnetic modes, similar to Planck's treatment of blackbody radiation. The geometry and dielectric functions of two macroscopic bodies give rise to a dispersion relation of allowed electromagnetic modes, which then yield the free energy of the system. The van der Waals force is derived by differentiation of the free energy with respect to separation. Both retardation effects and many-body effects are naturally incorporated in the formalism. Numerical results have been compared to measurements of van der Waals forces for a variety of materials.[4]

A central ingredient of the theory is the dielectric function of bulk materials at purely imaginary values of the frequency $\epsilon(i\xi)$. By the use of Kramers-Kronig relations, the complex dielectric function is determined from its imaginary part, $\epsilon''(\omega) \equiv \mathrm{Im}\,\epsilon(\omega)$.[5,6] The standard procedure[5,6] has been either to infer $\mathrm{Im}\,\epsilon(\omega)$ from the measured absorption spectrum or to model the dielectric response function by a collection of Lorentz harmonic oscillators. Only a few fragmentary theoretical attempts have been made to utilize the full frequency ω and wave-vector $\mathbf{k}$-dependent dielectric function $\epsilon(\omega,\mathbf{k})$[7] in the theory of dispersion forces for spatially dispersive media, such as electrolytes or molecular fluids.[8–10] These early attempts seldom carried out numerical calculations because of a lack of knowledge of $\epsilon(\omega,\mathbf{k})$ (either theoretical or experimental). In a recent review article by Barash and Ginzburg,[11] the spacial dispersion and nonlocality were taken into account from the very beginning in their discussion, but the wave-vector dependence was later neglected before giving concrete results.

We consider the configuration of two semi-infinite slabs separated by a thickness ℓ of order of 0.3–10 nm (and thus ignore retardation effects). In a pairwise summation theory that uses attractive potentials proportional to r^{-6}, where r is the distance between two particles, it can be shown that the interaction energy between two slabs is proportional to ℓ^{-2}. It is therefore customary to write the interaction energy per unit area between two slabs as

$$F = -\frac{A}{12\pi\ell^2},$$

where A is the Hamaker constant. Similarly, in Lifshitz's theory of dispersion forces, if one assumes the long-wavelength limit of dielectric functions, $\epsilon(\omega) \equiv \epsilon(\omega,\mathbf{k}\to 0)$, A is again a constant with respect to the separation ℓ. The most important contribution to the van der Waals interaction comes from electromagnetic modes with wave vectors $k \sim 1/\ell$. Because the first Brillouin zone of a crystalline solid is of the order of 10 nm^{-1}, it is common to use the dielectric function $\epsilon(\omega)$ in the long-wavelength limit. The usual rationale is that "*provided we are concerned with radiation of wavelength much larger than intermolecular spacings* ($\omega < 10^{18}$ rad s^{-1}), *the effect of the medium can be described by the dielectric response function* $\epsilon(\omega)$ *of the medium.*"[6] However, when the separation between two slabs is of the order of 1 nm, electromagnetic modes of wavelength comparable to interatomic spacings become important and it becomes necessary to consider the full dielectric function over the first Brillouin zone.

In this paper, we show that at distances of <2 nm, the full dielectric function over a wide range of frequencies and wave vectors has to be incorporated into the dispersion force theory. We first examine the formalism in a simple geometry (two half slabs), and then illustrate with a numerical example how the use of full dielectric functions $\epsilon(\omega,\mathbf{k})$ changes the values of Hamaker constants. When two slabs are separated by a short distance (e.g., $\sim$1 nm, which is still larger than

distances of appreciable charge overlap), the difference between resulting Hamaker constants using the macroscopic dielectric function $\epsilon(\omega)$ and the full $\epsilon(\omega,\mathbf{k})$ is as much as 30%. Our interest in these short separation distances stems from a need to determine forces necessary to exfoliate graphite into individual graphene sheets and to determine the colloidal interactions between stacks of graphene sheets.[12,13] We also point out that the full wave-vector-dependent dielectric function can give rise to anisotropic van der Waals forces.

II. THEORY

The extension of the theory of dispersion forces to wave-vector-dependent dielectric functions amounts to replacing $\epsilon(\omega)$ with the appropriate $\epsilon(\omega,\mathbf{k})$. Otherwise, our derivation largely follows the standard treatment[5,6,14] of the force between two macroscopic bodies. Throughout the discussion, the retardation effect will be neglected.

A. Free energy

If ω_j is the frequency of an electromagnetic (EM) mode, the free energy corresponding to the mode ω_j is

$$F_j = -k_B T \ln Z_j = k_B T \ln\left[2\sinh\left(\frac{\hbar\omega_j}{2k_B T}\right)\right]. \tag{1}$$

Summing over all the allowed frequencies, the free-energy contribution from the EM field is

$$F = k_B T \sum_j \ln\left[2\sinh\left(\frac{\hbar\omega_j}{2k_B T}\right)\right]. \tag{2}$$

To emphasize that frequency ω depends on wave vector $\mathbf{k}$, we write the free energy of the EM field of wave vector $\mathbf{k}$ as

$$F_{\mathbf{k}} = k_B T \sum_j \ln\left[2\sinh\left(\frac{\hbar\omega_j(\mathbf{k})}{2k_B T}\right)\right]. \tag{3}$$

Finally, the total free energy is given by

$$F = \sum_{\mathbf{k}} F_{\mathbf{k}}. \tag{4}$$

B. Dispersion relation $\mathcal{D}(\omega)$

We consider the simple geometry of two semi-infinite slabs separated by distance ℓ, as shown in Fig. 1.

The dielectric displacement $\mathbf{D}$ satisfies

$$\mathbf{D}(\omega,\mathbf{r}) = \int \epsilon(\omega,\mathbf{r},\mathbf{r}')\mathbf{E}(\omega,\mathbf{r}')d^3\mathbf{r}'.$$

We assume the dielectric function is homogeneous parallel to the slabs, and furthermore, it is local for the direction perpendicular to the slabs: $\epsilon(\omega,\mathbf{r},\mathbf{r}')=\epsilon(\omega,x-x',y-y',z)$ (some justification is given in Sec. II C). We take Fourier transforms and obtain

$$\mathbf{D}(\omega,\mathbf{k},z) = \epsilon(\omega,\mathbf{k},z)\mathbf{E}(\omega,\mathbf{k},z), \tag{5}$$

where $\mathbf{k}$ is a two-dimensional, transverse wave vector (k_x,k_y). From now on we will refer to $\mathbf{k}$ as a two-dimensional wave vector unless otherwise noted. Depending on the value of the position variable z, one can use the slab index s ($s=L,m,R$) to denote the left slab, medium, or right slab. The dielectric function can be diagonalized in the principal axes as a tensorial quantity

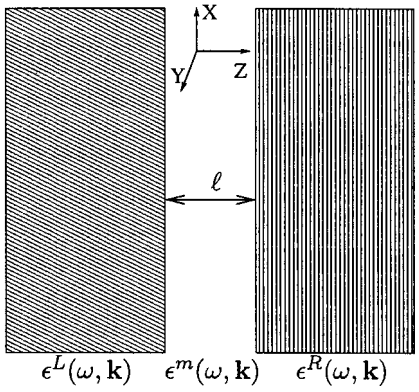

FIG. 1. Two semi-infinite slabs separated by distance ℓ. The two slabs can be made of different materials and have different orientations (represented by different shadings).

$$\epsilon^s_{ij}(\omega,\mathbf{k}) = \begin{pmatrix} \epsilon^s_x(\omega,\mathbf{k}) & 0 & 0 \\ 0 & \epsilon^s_y(\omega,\mathbf{k}) & 0 \\ 0 & 0 & \epsilon^s_z(\omega,\mathbf{k}) \end{pmatrix}. \tag{6}$$

Let ϕ_s be the spatial part of the scalar potential $\phi_s(x,y,z)\exp(-i\omega t)$ of the electric field $\mathbf{E}$. By setting $\mathbf{E}=-\nabla\phi$ (neglecting retardation effects), ϕ_s satisfies Laplace's equation in charge-free space

$$\nabla\cdot\mathbf{D} = ik_x D_x + ik_y D_y + \partial D_z/\partial z \tag{7}$$

$$= [k_x^2\epsilon^s_x(\omega,\mathbf{k}) + k_y^2\epsilon^s_y(\omega,\mathbf{k})]\phi_s - \epsilon^s_z(\omega,\mathbf{k})\partial^2\phi_s/\partial z^2 = 0. \tag{8}$$

In Eq. (8), we assume that ϵ^s is homogeneous in each slab, which amounts to neglecting $\nabla\epsilon^s\cdot\nabla\phi_s$. The inhomogeneity at the interface regions is also neglected. (In the long-wavelength limit, $\nabla\epsilon^s$ vanishes inside bulk materials.) After inserting a solution of the form,

$$\phi_s(x,y,z) = f_s(z)\exp[i(k_x x + k_y y)],$$

we obtain

$$\epsilon^s_z(k_x,k_y)f_s''(z) - [\epsilon^s_x(k_x,k_y)k_x^2 + \epsilon^s_y(k_x,k_y)k_y^2]f_s(z) = 0.$$

Let

$$\beta_s^2 = \frac{\epsilon^s_x(k_x,k_y)}{\epsilon^s_z(k_x,k_y)}k_x^2 + \frac{\epsilon^s_y(k_x,k_y)}{\epsilon^s_z(k_x,k_y)}k_y^2, \tag{9}$$

and we obtain a simplified equation

$$f_s''(z) - \beta_s^2 f_s(z) = 0. \tag{10}$$

In a homogeneous material, $\epsilon^s_x=\epsilon^s_y=\epsilon^s_z$, β_s becomes the magnitude of the wave vector $\mathbf{k}$ in the xy plane. The boundary conditions are that both ϕ_s and $D_z=-\epsilon^s_z(k_x,k_y)\partial\phi_s/\partial z$ are continuous at the interface. After imposing the boundary

conditions, we find that $\mathcal{D}(\omega,\mathbf{k})=0$ has to be satisfied

$$\mathcal{D}(\omega,\mathbf{k}) = 1 - \left(\frac{a-1}{a+1}\right)\left(\frac{b-1}{b+1}\right)e^{-2\beta_m \ell} = 0, \tag{11}$$

where

$$a = \frac{\epsilon_z^L(\omega,\mathbf{k})\beta_L}{\epsilon_z^m(\omega,\mathbf{k})\beta_m}, \quad b = \frac{\epsilon_z^R(\omega,\mathbf{k})\beta_R}{\epsilon_z^m(\omega,\mathbf{k})\beta_m}. \tag{12}$$

C. Interaction energy

Now we can evaluate the summation over all allowed frequencies in Eq. (3)

$$F_{\mathbf{k}} = k_B T \sum_j \ln\left[2\sinh\left(\frac{\hbar\omega_j(\mathbf{k})}{2k_B T}\right)\right] = k_B T \sum_{n=0}^{\infty}{}' \ln \mathcal{D}(i\xi_n,\mathbf{k}),$$

where $\xi_n = 2\pi n k_B T/\hbar$. The prime in the second summation above indicates that the $n=0$ term is to be multiplied by $1/2$. The second equality results from Cauchy's theorem of complex variables.[14]

Thus far, two major approximations were made. One is the neglect of retardation effects due to the finite speed of light. As a result, the slab separation ℓ is restricted to be smaller than c/ω_p, where c is the speed of light and ω_p is a characteristic collective mode frequency (in graphite, $\hbar\omega_p$ is 12.6 eV, therefore, ℓ should be <10 nm). The second approximation is our simplification of the dielectric functions near the interfaces. The approximation of an abrupt change in the dielectric function at the interface is valid for a quasi-two-dimensional material, such as graphite. If there is rearrangement of surface atoms or dangling bonds, a transition region of roughly the width of an atomic layer should be considered, as was done in Ref. 15. When the surface layer is much shorter than the slab separation ℓ, the inhomogeneity at surfaces can be neglected. The lack of periodicity in the direction perpendicular to the surface (the z direction) further complicates the study of dielectric response at interfaces. Although retardation effects can be readily incorporated,[14] a full treatment of dielectric functions at crystal surfaces involves local-field effects and other complications, which we will not consider here.[16]

To include *all* possible values of the transverse wave vector $\mathbf{k}$, we perform the integration

$$F = k_B T \sum_{n=0}^{\infty}{}' \int_{-\infty}^{\infty}\frac{dk_x}{2\pi}\int_{-\infty}^{\infty}\frac{dk_y}{2\pi} \ln \mathcal{D}(i\xi_n,k_x,k_y) \tag{13}$$

$$= \frac{k_B T}{4\pi^2}\sum_{n=0}^{\infty}{}' \int_{-\infty}^{\infty} dk_x dk_y \ln\left[1 - \left(\frac{a-1}{a+1}\right) \times \left(\frac{b-1}{b+1}\right)e^{-2\beta_m \ell}\right]. \tag{14}$$

The interaction free energy can be written as

$$F = -\frac{A(\ell)}{12\pi\ell^2}, \tag{15}$$

where $A(\ell)$ is

$$A(\ell) = -\frac{3\ell^2 k_B T}{\pi}\sum_{n=0}^{\infty}{}' \int_{-\infty}^{\infty} dk_x dk_y \ln\left[1 - \left(\frac{a-1}{a+1}\right) \times \left(\frac{b-1}{b+1}\right)e^{-2\beta_m \ell}\right]. \tag{16}$$

D. van der Waals force and Hamaker constants

When ℓ is much larger than the lattice constant of the slabs, the exponential factor $\exp(-2\beta_m\ell)$ will single out the long-wavelength component in Eq. (16), and we may use the limit of Eq. (12)

$$\tilde{a} = \frac{\epsilon_z^L(i\xi_n)\beta_L}{\epsilon_z^m(i\xi_n)\beta_m}, \quad \tilde{b} = \frac{\epsilon_z^R(i\xi_n)\beta_R}{\epsilon_z^m(i\xi_n)\beta_m}. \tag{17}$$

In a homogeneous cubic system, $\beta_m = k = \sqrt{k_x^2 + k_y^2}$. By a change of variables ($x = 2\beta_m\ell$), we obtain the classical result for the Hamaker constant A

$$A = -\frac{3k_B T}{2}\sum_{n=0}^{\infty}{}' \int_0^{\infty} x dx \ln\left[1 - \left(\frac{\tilde{a}-1}{\tilde{a}+1}\right)\left(\frac{\tilde{b}-1}{\tilde{b}+1}\right)e^{-x}\right], \tag{18}$$

$$= \frac{3k_B T}{2}\sum_{m=1}^{\infty}\sum_{n=0}^{\infty}{}' \int_0^{\infty} x e^{-mx}\frac{1}{m}\left(\frac{\tilde{a}-1}{\tilde{a}+1}\right)\left(\frac{\tilde{b}-1}{\tilde{b}+1}\right)dx. \tag{19}$$

Usually the first few terms in the expansion of the logarithm suffice to obtain a converged result. The weight function in Eq. (19), $x\exp(-mx)$, is centered at $x = 1/m$ or $k = (2m\ell)^{-1}$. The condition that ℓ is much larger than the lattice constant allows us to set $k = (2m\ell)^{-1} \to 0$ in Eq. (12). The nonretarded Hamaker function $A(\ell)$ approaches a constant *only* in the above limit. When we use the more general form [Eq. (12)], the Hamaker function actually depends on the separation ℓ. As ℓ decreases, the effective screening is reduced and the Hamaker function $A(\ell)$ decreases.

Only the long-wavelength limit of dielectric function, $\epsilon(\omega) = \epsilon(\omega,\mathbf{k}\to 0)$, has been extensively used.[5,6] This approximation becomes valid only for ℓ much larger than the interatomic separation, which is typically about 0.2 nm. For a broad range of separations (up to 2 nm for graphite), the theory requires the use of the complete dielectric function $\epsilon(\omega,\mathbf{k})$, contrary to common practice. In Sec. III, we will demonstrate this by a numerical example.

There is no orientational dependence of the van der Waals interaction when the macroscopic (long-wavelength limit) dielectric function $\epsilon(\omega)$ is isotropic. However, anisotropy can arise from the directional dependence of $\epsilon(\omega,\mathbf{k})$ at nonzero $\mathbf{k}$. The current approach can be extended to compute anisotropic van der Waals forces resulting from the directional dependence of the wave vector $\mathbf{k}$ in $\epsilon(\omega,\mathbf{k})$. The anisotropic van der Waals force may provide the driving force for orientational adsorption on crystal surfaces.[17,18] The formalism and numerical calculation have been carried out recently and will be published elsewhere.[19]

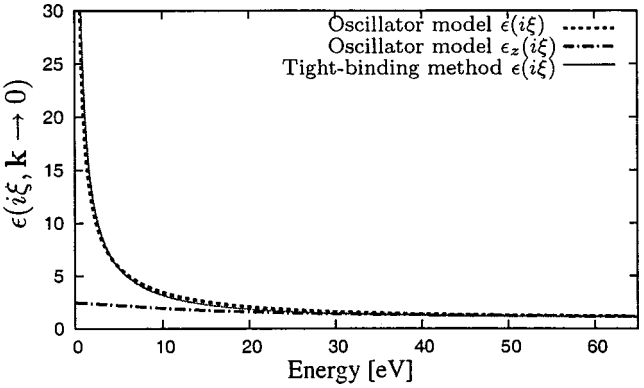

FIG. 2. Comparison of the real part of the dielectric function $\epsilon(i\xi,\mathbf{k}\to 0)$ at imaginary frequency ξ from the oscillator model[20] and from the tight-binding method (wave vector $|\mathbf{k}|=0.8\ \mathrm{nm}^{-1}$). The in-plane dielectric function $\epsilon(i\xi)$ from the oscillator model (dotted line) and the tight-binding method (solid line) are in excellent agreement. The dielectric function perpendicular to the basal plane (shown as a dotted-dashed line) $\epsilon_z(i\xi)$ is smaller than the in-plane dielectric function and has only weak wave-vector dependence.

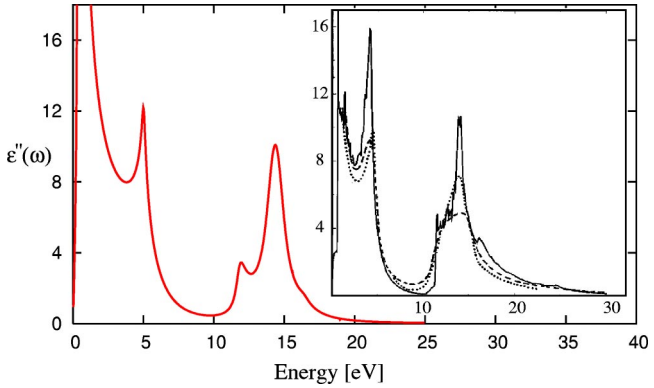

FIG. 3. $\epsilon''(\omega,\mathbf{k}=0)$ obtained using the tight-binding method (thick line) in the present work. The inset shows the dielectric function $\epsilon''(\omega,\mathbf{k}=0)$ of graphite from optical measurements (dotted line[23] and dashed line[24]) and first-principles calculation (solid line).[22]

III. NUMERICAL EXAMPLE: GRAPHITE

We illustrate the use of full wave-vector-dependent dielectric functions in two physical systems: graphite-air-graphite and graphite-water-graphite. Graphite is a quasi-two-dimensional crystal. Owing to the large interlayer distance and weak interlayer interaction, the dielectric function perpendicular to the basal plane (extraordinary z axis) has only a weak wave-vector dependence [$\epsilon_z(\omega)$ is close to 1 for all frequencies; see Fig. 2]. Therefore it suffices to treat $\epsilon_z(\omega)$ by the oscillator model,[20] and most of the computational effort will be focused on the calculation of the in-plane dielectric function. Within the random-phase approximation, the in-plane dielectric function $\epsilon(\omega,\mathbf{k})$ of a two-dimensional graphite layer is given by

$$\epsilon(\omega,\mathbf{k}) = 1 - \frac{4\pi e^2}{k}\sum_{n,n'}\int_{1\mathrm{st\ BZ}}\frac{d^2\mathbf{q}}{(2\pi)^2}|\langle n',\mathbf{q}+\mathbf{k}|e^{i\mathbf{k}\cdot\mathbf{r}}|n,\mathbf{q}\rangle|^2 \times\frac{f(E_{n',\mathbf{q}+\mathbf{k}})-f(E_{n,\mathbf{q}})}{E_{n',\mathbf{q}+\mathbf{k}}-E_{n,\mathbf{q}}-(\hbar\omega+i\Gamma)}, \quad (20)$$

where f is the Fermi distribution function. The summation of n,n' is over valence and conduction bands, Γ represents broadening in the absorption spectrum, and the integration is over crystal momentum $\mathbf{q}$ within the first Brillouin zone. The calculation can be carried out either for a tight-binding model[21] or with a first-principles method.[22] In the present work, we adopt the tight-binding approach, which is more computationally efficient. For materials for which tight-binding parameters are not available, the full dielectric function can be computed by first-principles calculations. Figure 3 shows the measured $\epsilon''(\omega)$[23,24] together with results from a first-principles calculation[22] and from the tight-binding method. Another method to obtain the dielectric function is by the oscillator model, which was fitted to experimental data.[20] In Fig. 2, the agreement between the tight-binding method and the oscillator model is excellent for the in-plane dielectric function. We plot $\epsilon''(\omega,\mathbf{k})$ and $\epsilon(i\xi,\mathbf{k})$ of graphite at several wave vectors $\mathbf{k}$ in Fig. 4. As can be expected from Eq. (20), the magnitude of $\epsilon(i\xi,\mathbf{k})$ decreases with the increasing wave vector $|\mathbf{k}|$. The reduced dielectric screening at finite wave vectors gives rise to a separation-dependent Hamaker function in Eq. (15) (even within the nonretarded limit).

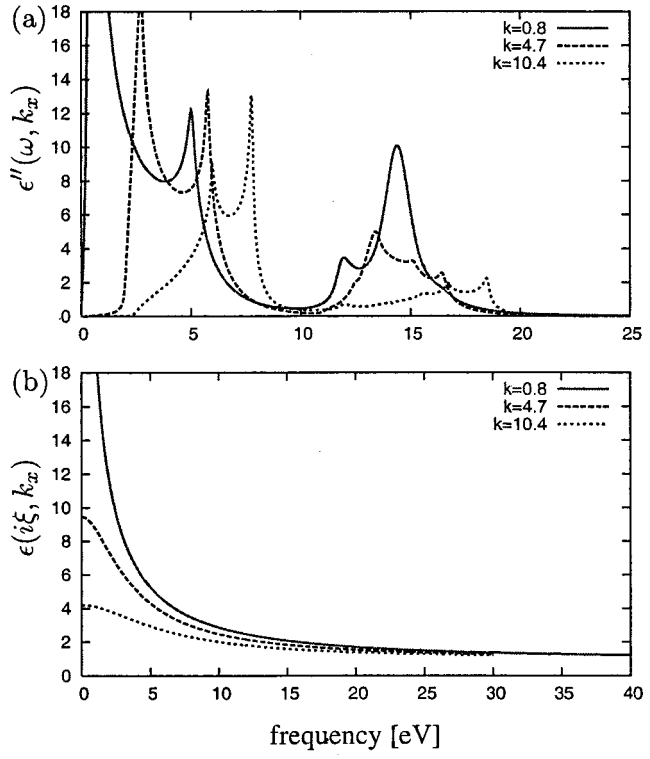

FIG. 4. (a) The dielectric function $\epsilon''(\omega,k_x)$ of graphite from a tight-binding calculation. Results are shown for wave vectors at $\mathbf{k}=k\hat{x}=0.8$, 4.7, and 10.4 nm^{-1}. (b) The dielectric function $\epsilon(i\xi,k_x)$ plotted vs imaginary frequency ξ.

TABLE I. Comparison between the experimental and theoretical Hamaker "constants" $A(\ell)$ (unit: 10^{-19} J). In the present work, the frequency-mode summation is done up to an ultraviolet cutoff (10^{17} rad Hz) and the temperature is set to room temperature 300 K.

	Full $\epsilon(i\xi,\mathbf{k})$ ($\ell=0.5$ nm)	Full $\epsilon(i\xi,\mathbf{k})$ ($\ell=1.0$ nm)	$\epsilon(i\xi,\mathbf{k}\to 0)$ ($\ell\to\infty$)	Experiments	Other theoretical results[25]
graphite-water-graphite	0.72	0.87	0.99	0.5-1.0[26]	1.15
graphite-air-graphite	1.82	2.03	2.20	2.1-5.9[27]	2.53

In Table I, we give values of the Hamaker function of two configurations, graphite-air-graphite and graphite-water-graphite. In general, using the full dielectric function $\epsilon(i\xi,\mathbf{k})$ results in a smaller Hamaker function. This is because at larger wave vectors, the screening is not as effective as it is in the $\mathbf{k}\to 0$, long-wavelength limit. Figure 5 shows the dependence of the Hamaker function on the separation ℓ in a graphite-air-graphite geometry. Our results for Hamaker constants in the long-wavelength limit are similar to those of previous calculations.[25] On the other hand, the experimentally measured values shown in Table I span a large range. In addition to the difficulty of precision measurement and of sample quality (samples of carbon black were used), this spread of values may reflect the separation dependence of the Hamaker function, as indicated in Fig. 5.

An interesting application of the above results is to a slab made of intercalated or exfoliated graphite. We model this system as a composite semi-infinite slab composed alternatively of a graphene sheet and a layer of water, as shown in Fig. 6. In intercalated graphite, the d spacings between two graphene sheets are increased from 0.34 nm (the spacing for thermodynamically stable graphite) to the thickness of one or several monolayers of water. Since the relevant wavelength of the EM mode is at least $\sim$3 nm (corresponding to the ultraviolet cutoff frequency), both intercalated water layers and graphene sheets have to be accounted for in setting up the boundary conditions, Eqs. (9)–(11). In general, the dielectric constant is $\epsilon=1+4\pi\chi$, where χ is the susceptibility. In a first-order approximation, χ is the sum of the polarizabilities of the constituent subsystems. Experimentally, graphite has to be oxidized in order to facilitate intercalation and the entry of water in between the layers. For simplicity, we assume no chemical reactions between intercalated water and graphene; then the electronic polarizability of layered materials is additive among its constituent layers. Thus, the dielectric tensor ϵ_c of composite slabs can be written as

$$\epsilon_c(\omega,\mathbf{k})_{\text{in-plane}}-1=r_g\cdot[\epsilon_g(\omega,\mathbf{k})_{\text{in-plane}}-1]+r_w\cdot[\epsilon_w(\omega)-1], \tag{21}$$

$$\epsilon_c(\omega,\mathbf{k})_z-1=r_g\cdot[\epsilon_g(\omega,\mathbf{k})_z-1]+r_w\cdot[\epsilon_w(\omega)-1], \tag{22}$$

where r_g (r_w) is the volume ratio of graphene (water) in the composite slab and $\epsilon_g(\omega,\mathbf{k})$ [$\epsilon_w(\omega)$] is the dielectric tensor of graphite (water).[28] Figure 7 shows the Hamaker constants of two semi-infinite intercalated graphite slabs with one or two monolayers of water. For the intercalated graphite with one monolayer of water, the Hamaker constant is 0.5×10^{-19} J, smaller than the similar graphite-water-graphite configuration (2.2×10^{-19} J). We remark that the reduction of the Hamaker function at short separations ($\sim$1 nm) is quite significant for intercalated graphite ($\sim$30% at 0.5 nm separation). Thus, when dispersing stacks of exfoliated graphene sheets colloidally, the magnitude of van der Waals interactions should be lower than that predicted by the conventional approach.

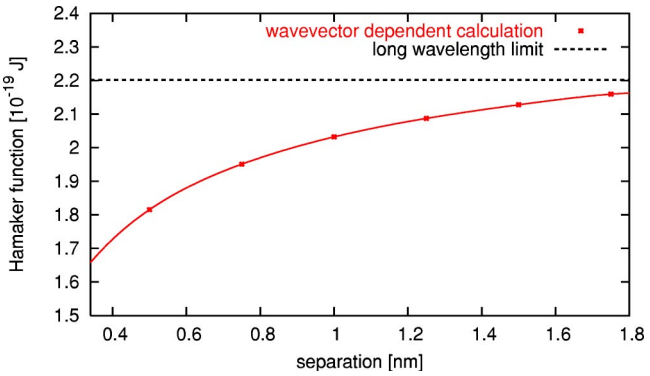

FIG. 5. The Hamaker function $A(\ell)$ for the graphite-air-graphite configuration. As the separation ℓ increases, the Hamaker function approaches its long-wavelength limit.

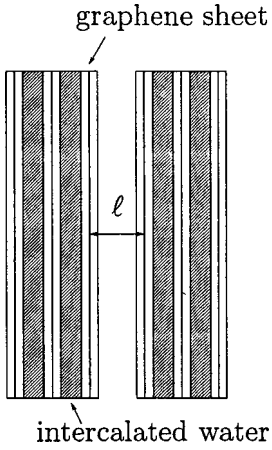

FIG. 6. Two semi-infinite identical composite slabs (intercalated graphite) separated by distance ℓ filled with water. The composite slab is composed alternatively of a graphene sheet and a layer of water. The centerline of the graphene layer indicates the position of carbon atoms.

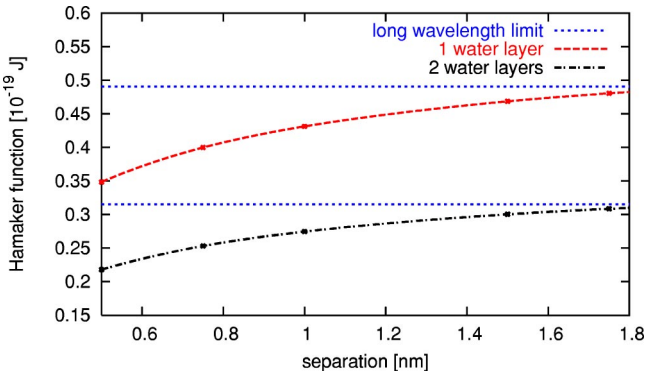

FIG. 7. The Hamaker function $A(\ell)$ for the intercalated graphite-water-intercalated graphite configuration. We used the volume ratio $r_g=0.45$ when there is one monolayer of water between two graphene sheets, and $r_g=0.62$ when there are two monolayers of water in-between. The Hamaker function approaches its long-wavelength limit at large separation ($\sim$1.8 nm).

IV. SUMMARY

To summarize, we have extended the use of dielectric functions in dispersion-force theory to include the wave-vector dependence of the dielectric. The Hamaker function $A(\ell)$ between two semi-infinite slabs is defined as

$$F = -\frac{A(\ell)}{12\pi\ell^2}.$$

Previous calculations showed that $A(\ell)$ is a constant within the nonretarded region. [$A(\ell)$ decreases when ℓ extends into the retarded region.] Our analysis reveals that this traditional description is valid only when ℓ is much larger than the interatomic separation. The use of full dielectric functions reveals a separation-dependent Hamaker function in the nonretarded region. For example, the Hamaker function between two graphite slabs diminishes significantly when the separation is less than about 2 nm. We explicitly show how to apply the formalism to compute the interaction energy between two graphite slabs and intercalated or exfoliated graphite slabs. The treatment can also be extended to study more general cases when the dielectric function is anisotropic because of the directional dependence of the wave vector $\mathbf{k}$ in $\epsilon(\omega,\mathbf{k})$. We hope the present work will encourage additional experiments and analysis to resolve the remaining discrepancies between theory and experiment.

ACKNOWLEDGMENTS

This work was supported by the NASA University Research, Engineering, and Technology Institute on BioInspired Materials (BIMat) under Award No. NCC-1-02037 and the National Science Foundation (MRSEC program) through the Princeton Center for Complex Materials (DMR 0213706).

[1] H. C. Hamaker, Physics (N.Y.) **4**, 1058 (1937).
[2] E. M. Lifshitz, Sov. Phys. JETP **2**, 73 (1956).
[3] I. E. Dzyaloshinski, E. M. Lifshitz, and L. P. Pitaevski, Adv. Phys. **10**, 165 (1961).
[4] L. Bergström, Adv. Colloid Interface Sci. **70**, 125 (1997).
[5] W. B. Russel, D. A. Saville, and W. R. Schowalter, *Colloidal Dispersions* (Cambridge University Press, Cambridge, England, 1992).
[6] R. J. Hunter, *Foundations of Colloid Science*, 2nd ed. (Oxford University Press, Oxford, 2001) Sec. 11.6.
[7] See, for example, J. M. Ziman, *Principles of the Theory of Solids*, 2nd ed. (Cambridge University Press, Cambridge, England, 1972).
[8] R. K. Bullough, J. Phys. A **3**, 751 (1970).
[9] B. Davies and B. W. Ninham, J. Chem. Phys. **56**, 5797 (1972).
[10] R. A. Craig, J. Chem. Phys. **58**, 2988 (1973).
[11] Y. S. Barash and V. L. Ginzburg, *The Dielectric Function of Condensed Systems* (North-Holland, Amsterdam, 1989).
[12] K. S. Novoselov, A. K. Geim, S. V. Morozov, D. Jiang, Y. Zhang, S. V. Dubonos, I. V. Grigorieva, and A. A. Firsov, Science **306**, 666 (2004).
[13] In a recent study by A. Abdala, D. H. Adamson, M. Herrera-Alonso, I. A. Aksay, and R. K. Prud'homme (unpublished), it has been shown that graphite can be exfoliated through rapid thermal expansion of water intercalated in between graphene sheets.
[14] J. Mahanty and B. W. Ninham, *Dispersion Forces* (Academic Press, London, 1976).
[15] V. A. Parsegian and G. H. Weiss, J. Colloid Interface Sci. **40**, 35 (1972).
[16] R. Del Sole and E. Fiorino, Phys. Rev. B **29**, 4631 (1984).
[17] E. J. Wanless and W. A. Ducker, J. Phys. Chem. **100**, 3207 (1996).
[18] C. L. Brown, I. A. Aksay, D. A. Saville, and M. H. Hecht, J. Am. Chem. Soc. **124**, 6846 (2002).
[19] J. Chun, J.-L. Li, R. Car, I. A. Aksay, and D. A. Saville (unpublished).
[20] A. B. Djurišić and E. H. Li, Am. J. Phys. **85**, 7404 (1999).
[21] M. F. Lin, C. S. Huang, and D. S. Chuu, Phys. Rev. B **55**, 13961 (1997).
[22] R. Ahuja, S. Auluck, J. M. Wills, M. Alouani, B. Johansson, and O. Eriksson, Phys. Rev. B **55**, 4999 (1997).
[23] E. A. Taft and H. R. Philipp, Phys. Rev. **138**, A197 (1965).
[24] K. Zeppenfeld, Chem. Eng. Prog. **243**, 229 (1971).
[25] R. R. Dagastine, D. C. Prieve, and L. R. White, J. Colloid Interface Sci. **249**, 78 (2002).
[26] P. A. Hartley and G. D. Parfitt, Langmuir **1**, 651 (1985).
[27] G. D. Parfitt and N. H. Picton, Trans. Faraday Soc. **64**, 1955 (1968).
[28] In the current study, the dielectric constant of bulk water is used for intercalated water layers, although water confined between graphene sheets can have quite different physical properties from bulk water [T. M. Truskett, P. G. Debenedetti, and S. Torquato, J. Chem. Phys. **114**, 2401 (2001)].